Atom Indonesia

Journal homepage: http://aij.batan.go.id

Calculated Electronic Energy Loss of Heavy Ions at Low Energies in LR-115, Kapton, SiO_2, and Al_2O_3 Amorphous Materials

J. El Asri[1], O. El Bounagui[2*], N. Tahiri[3], A. Chetaine[1], H. Erramli[4]

[1]*Nuclear Reactor, Nuclear security and Environment, Faculty of Sciences, Mohammed V University in Rabat, 4 Avenue Ibn Batouta B.P. 1014 RP, Rabat, Morocco*
[2]*EPHE-SM, Faculty of Sciences, Mohammed V University in Rabat, 4 Avenue Ibn Batouta B.P. 1014 RP, Rabat, Morocco*
[3]*LaMCScl, Faculty of Sciences, Mohammed V University in Rabat, 4 Avenue Ibn Batouta B.P. 1014 RP, Rabat, Morocco*
[4]*Faculty of Science Semlalia, University Cadi Ayyad Marrakech, BP 511 Avenue Prince Abdellah Marrakech, Morocco*

ARTICLE INFO

Article history:
Received 17 July 2020
Received in revised form 2 December 2020
Accepted 3 December 2020

Keywords:
Electronic stopping power;
Modified LSS theory;
Heavy ions;
Polymeric foils

ABSTRACT

The electronic stopping powers of LR-115 and Kapton polymeric foils have been estimated, using Monte Carlo simulations, for ^{9}Be, ^{11}B, ^{12}C, ^{14}N, ^{16}O, and ^{35}Cl ions covering the energy range ~0.1-1.0 MeV/n. Comparison of stopping power based on Lindhard, Scharff, and Schiott (LSS) theory with the corresponding values obtained by SRIM and MSTAR codes in LR-115 and Kapton polymeric foils illustrate a significantly large deviations. However, a semiempirical equation has been proposed here and tested for better stopping power calculations at low-energy regime in the domain of LSS theory for Z = 4-8 ions across materials. Furthermore, the electronic energy losses for ^{9}Be and ^{16}O ions in SiO_2 and Al_2O_3, respectively, have been calculated in the energy range of ~0.1-1.0 MeV/n. The calculated stopping powers exhibit up to 10 % deviation from the experimental values and MSTAR data.

INTRODUCTION

The LSS theory was developed by Lindhard, Scharff, and Schiott [1] to calculate and evaluate the electronic energy loss at low energies. However, the deceleration and scattering of charged particle in matter is considerably used in several techniques and phenomenon of physics such as: ion channeling, radiation damage, sputtering, the reflection and transmission of charged particles, and charged particle activation analysis [2,3]. At low energies, the Bethe formula [4] cannot be used to calculate the electronic energy loss, because the inner-shell contribution to the energy loss is relatively negligible. In fact, the energy loss becomes proportional to the velocity of the projectile. Experimental and theoretical studies have been investigated on the electronic energy loss for different ions and target materials [5-7]. Moreover, the Monte Carlo simulation (MCs) has a number of advantages in comparison to analytical formulations based on the transport theory [8-10]. Furthermore, the electronic energy loss of light and heavy ions in compound materials have attracted attention in recent years [11-14] due to their increasing use in ion beam applications and materials science. Several measurements of the energy loss have been conducted and compared with the calculated values for heavier ions [15]. Also, many experiments have been conducted to determine the electronic stopping power for different heavy ions with Z_1 = 5 to 29 in silicon dioxide and various polymeric materials such as polyethylene terephthalate or PET $(C_{10}H_8O_4)_n$, polycarbonate/PC $(C_{16}H_{14}O_3)_n$, and polyethylene naphthalate/PEN $(C_{14}H_{10}O_4)_n$ [16]. In a previous paper, calculations of the stopping power data of the heavy ions of ^{19}F, ^{23}Na, ^{24}Mg, ^{27}Al, ^{28}Si, ^{31}P, ^{32}S, ^{35}Cl, and ^{40}Ar were reported for Formvar and Mylar polymeric materials for the 0.1 to 1.0 MeV/n energy region [17]. More experiments are needed for various ions and stopping targets to draw a definite conclusion about the usefulness of the LSS theory in the low-energy region. Until it is definitely

*Corresponding author.
E-mail address: elbounagui@gmail.com
DOI: https://doi.org/10.17146/aij.2021.1080

confirmed, we recommend the use of the modified LSS for low-energy ions.

In the present work, we investigate the electronic energy loss in amorphous materials (cellulose nitrate LR-115, Kapton polyimide film, SiO_2, and Al_2O_3) for different incident charged particles, such as ^{9}Be, ^{11}B, ^{12}C, ^{14}N, ^{16}O, and ^{35}Cl ions, at low velocities using Monte Carlo simulations and modified LSS theory. Also, all results obtained by Monte Carlo simulations and modified LSS theory are compared with those calculated by SRIM and MSTAR computer codes and experimental values.

EXPERIMENTAL METHODS

The electronic energy loss for $v \leq v_0 Z_1^{2/3}$, where v_0 and Z_1 are the Bohr velocity and incident atomic number, respectively, as described by LSS theory for heavy ions at low energies can be given by (1).

$$(S_e)_{LSS} = \zeta_e 8\pi e^2 a_0 N Z_1^{2/3} \left(\frac{Z_1 Z_2}{Z}\right) V_r \quad (1)$$

In (1), ζ_e represents the correlation factor (equal to $Z_1^{1/6}$, while N and a_0 denote the atomic density and atomic radius, respectively. Z_2 is the target atomic number and v_r is an ion reduced velocity given by:

$$v_r = \frac{v}{v_0 Z_1^{2/3}} \text{ and } Z = (Z_1^{2/3} + Z_2^{2/3})^{3/2}$$

The electronic energy loss given by LSS formula [1] contain the constant ζ_e that is approximately equal to $Z_1^{1/6}$. This factor ζ_e is not only dependent on the ion atomic number Z_1 but also on the target atomic number Z_2. In this case ζ_e can be rewritten as (2), where a = 0.956, b = -0.573, and c = 0.237.

$$\zeta_e' = a(Z_1^b Z_2^c) \quad (2)$$

We have attempted to include a semiempirical formula by taking into account, in our calculation approach, the concept of effective charge of moving ions and the exponential fit function [17]. Based on the previous work, through this study we propose the following equation to evaluate the electronic stopping power $(S_e)_{LSS}$ for heavy ions traversing the targets at low-energy region [17]. $(S_e)_{Modified\text{-}LSS}$ is given as (3).

$$(S_e)_{Modified-LSS} = (S_e)'_{LSS} \times f(E) \quad (3)$$

In (3), $(S_e)'_{LSS}$ and $f(E)$ are defined by Eqs. (4) and (5):

$$(S_e)'_{LSS} = \zeta_e' \times (S_e)_{LSS} \quad (4)$$

$$f(E) = a_1 e^{-b_1 E} \quad (5)$$

In (5), a_1 and b_1 are adjustable parameters and are taken as follows:
$1.587 < a_1 < 1.993$ and $2.301 < b_1 < 2.549$.
However, the expression of Eq. (3) can be given as in (6).

$$(S_e)_{Modified-LSS} = \zeta_e' 8\pi e^2 a_0 N Z_1^{2/3} \left(\frac{Z_{1eff} Z_2}{Z}\right) \left(\frac{V}{V_0}\right) \left(a_1 e^{(-b_1 E)}\right) \quad (6)$$

The semiempirical expression suggested as Eq. (5) can be considered as a function of incident ion energy E. The empirical values for a_1 and b_1 that would fit the calculation of stopping power data need to be determined.

However, at low energies, the electronic energy loss becomes proportional to ion velocity. In this case, it is considered to use an energy loss which is correlated with the impact parameter of each collision (see Fig. 1). The transfer energy in the collision is given by (7), where σ is the cross section of interaction and b is the impact parameter.

$$\langle T \rangle = \int_{b_{min}}^{b_{max}} T(\sigma) d\sigma \quad (7)$$

Here, a typical interaction is considered. The target is described by assuming a cylinder with radius equal to the impact parameter b_{max} and length L. The average free flight path can then be calculated by (8).

$$b^2 \pi l = N^{-1} \quad (8)$$

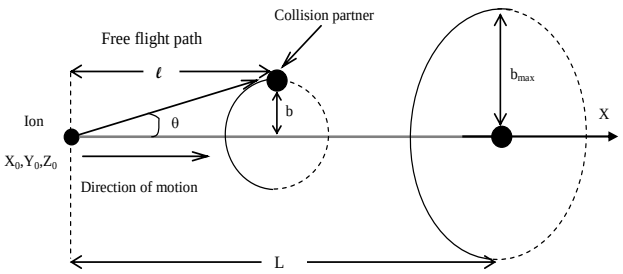

Fig. 1. Schematic of collision between ions and target.

The target is sufficiently thin (a few microns). The program generates a homogeneous distribution of particle position (X,Y,Z) in a cylinder characterized by radius b_{max}, which represent the bombarded volume.

Triplets of numbers ξ_1, ξ_2, and ξ_3 were generated by using a program called Random

Subroutine on a congruential method [7,18], where ξ_i is a random number ($0 \leq \xi_i < 1$).

$$\xi_1 = \text{random}(t_1) \quad (9)$$
$$\xi_2 = \text{random}(t_2) \quad (10)$$
$$\xi_3 = \text{random}(t_3) \quad (11)$$

Here, X is generated homogeneously in the interval [0, L], using a random sampling procedure.

$$X = \xi_1 L \quad (12)$$

Homogeneously-distributed {Y, Z} couples in a circle of radius b_{max} is obtained by generating {Y, Z} couples isotropically in a square of $2b_{max}$ sides, with $Y \in [-b_{max}, b_{max}]$ and $Z \in [-b_{max}, b_{max}]$ by (13 and 14).

$$Y = -b_{max} + 2b_{max}\xi_2 \quad (13)$$
$$Z = -b_{max} + 2b_{max}\xi_3 \quad (14)$$

The isotropic generation of the couple {Y, Z} in the circle of radius b_{max} is obtained by the test (15).

$$Y^2 + Z^2 \leq b_{max}^2 \quad (15)$$

The emission angle is generated using random sampling procedure [17,19]. Our program uses the angular distribution of ions collision in the laboratory frame, where θ is randomly calculated by using relation (16) [20], where ξ_4 is a random number ($0 \leq \xi_4 < 1$).

$$\theta = \arccos(1 - 2\xi_4) \quad (16)$$

Each ion is characterized by the parameters which are the identifier, the atomic number, the atomic mass, the energy, the direction and the three-dimensional Cartesian coordinate. The evolution of these parameters can be followed using Monte Carlo simulation [7,17,21]. The particle is assumed to change direction as a result of binary electronic collisions and moves in a straight path between two consecutive collisions. The energy of the particle is reduced as a result of electronic collision, and a trajectory is terminated either when the energy drops below a prespecified value or when the particle position is outside the target. The target is assumed to be amorphous with atoms at random locations and the directional properties applicable for a crystalline material being ignored [3,10]. This program calculates the final three-dimensional distributions of the ions, the energy transfer, the energy loss, and the electronic stopping power. The trajectory is stopped when the ion energy is smaller than I (mean excitation energy). A conventional simulation run was performed with such a high number of ion trajectories (1 000 000) that statistical fluctuations are negligible.

Table 1 illustrates the values of average atomic number Z_2, average atomic weight A_2, and mean excitation energy I. To calculate the average mean excitation energy, (17) can be used [8,22].

$$\ln(I) = \frac{\sum_i n_i Z_i \ln(I_i)}{\sum_i n_i Z_i} \quad (17)$$

In (17), I_i, Z_i, and n_i denote the mean excitation energy, atomic number, and atomic concentration of the ith component of the composite target material, respectively.

Table 1. Averages of atomic number Z_2, atomic weight A_2, and mean excitation energy I for target materials used.

Target	Z_2	A_2	I (eV)
Kapton	5.03	9.80	80.13
LR-115	5.20	10.08	83.07
SiO_2	9.99	19.99	130.69
Al_2O_3	10	20.40	132.07

RESULTS AND DISCUSSION

It is useful to study the effect of correlation factor included in Eq. (1) and the exponential function on the behavior of electronic energy loss for several different incident charged particle species, namely Be, B, C, N, and O ions, in amorphous targets. These behaviors are illustrated in Figs. 2(a) and 2(b). From Fig. 2(a), it is found that, in absence of the correlation factor, the electronic energy loss increases with increasing energy. In this energy region, the electronic stopping power is proportional to the ion velocity and for systems with different atomic numbers $Z_1 \neq Z_2$. On the other hand, Fig. 2(b) shows that in the presence of the correlation factor and exponential function, as given by Eq. (5), the electronic energy loss increases with increasing incident energy until it reaches a maximum and then decreases.

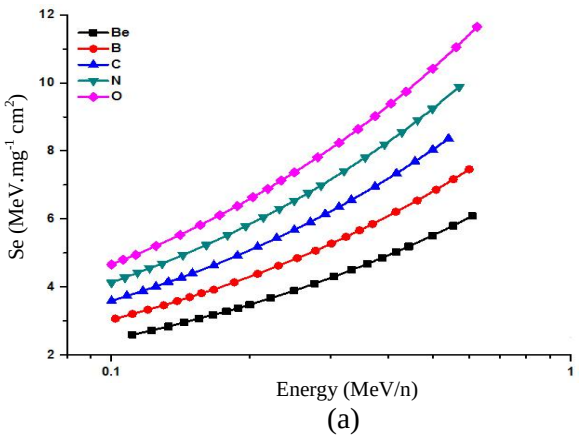

(a)

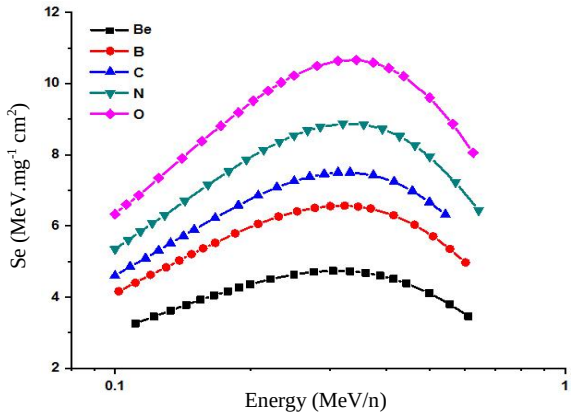

(b)

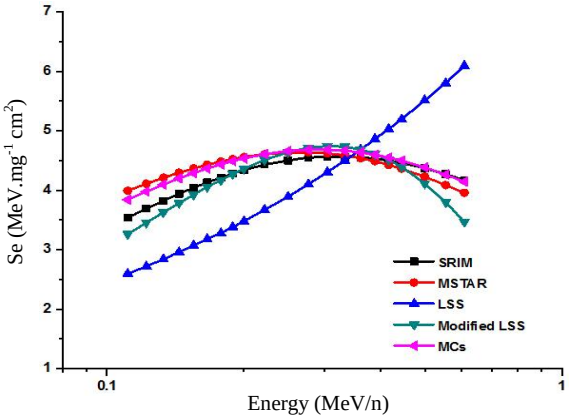

(a)

Fig. 2. The electronic energy loss as a function of incident ions energy for different heavy ions in Kapton polyimide film $(C_{22}H_{10}O_5N_2)_n$ polymeric foil. (a) LSS theory and (b) modified LSS theory.

In Figs. 3 and 4, the corresponding behavior of electronic energy loss as a function of energy in Kapton and LR-115 are plotted for the aforespecified charged particles at low energy. In Figs. 3(a)-(e) and Figs. 4(a)-(e), the calculated electronic stopping power values of Be, B, C, N, and O ions in Kapton and LR-115 based on modified LSS theory formula given by Eq. (6) and Monte Carlo simulations in the energy range of ~0.1-0.5 MeV/n provide a close agreement with those calculated by SRIM and MSTAR codes. However, a significant discrepancy has been observed between the values calculated by the LSS equation in (1) and those obtained using Monte Carlo simulations, modified LSS theory expression in Eq. (6), SRIM code, and MSTAR code. In the range of energy ~0.1-1.0 MeV/n, the LSS formula considerably underestimates with our calculation values. The deviation of LSS theory calculate values from Monte Carlo simulations and modified LSS theory vary from 20 % to 25 %. It is apparent from Figs. 3(a)-(e) and Figs. 4(a)-(e) that the calculated electronic stopping power data using the modified LSS theory formula in Eq. (6) are in close agreement with SRIM and MSTAR electronic stopping power values in solid targets of Kapton and LR-115. In this case, the calculated values of electronic stopping power using Monte Carlo simulations present an excellent agreement in the energy range of ~0.1-1.0 MeV/n. Also, a small deviation is observed when the calculated values are compared with data from SRIM (about 6 %) and from MSTAR (about 9 %).

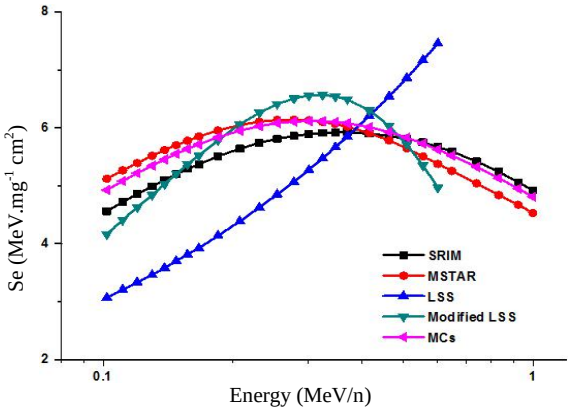

(b)

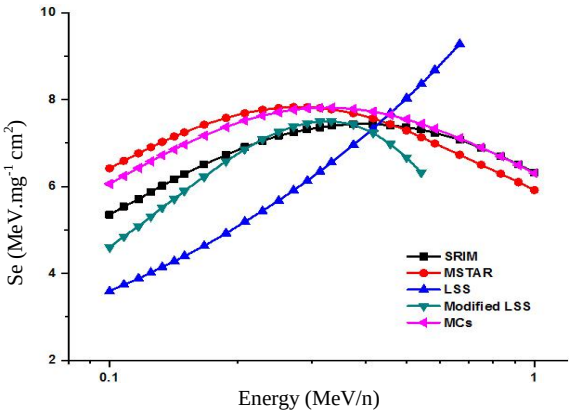

(c)

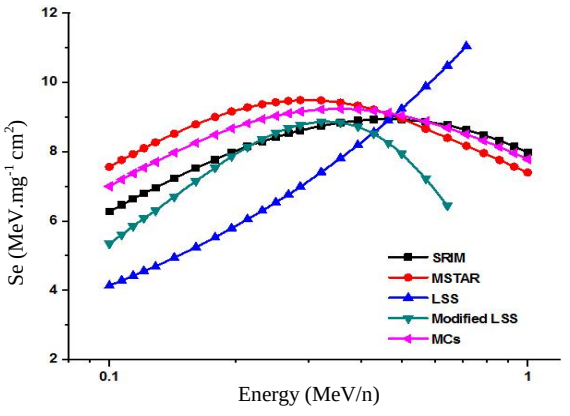

(d)

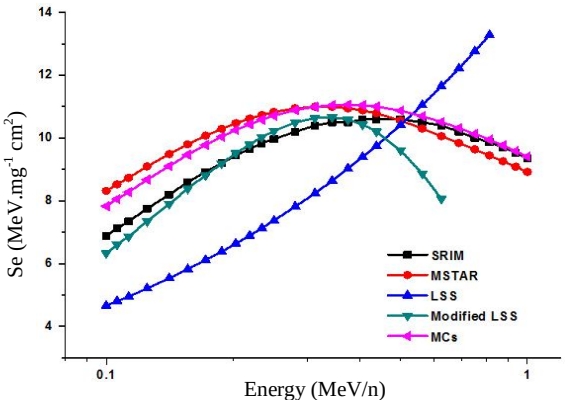

(e)

Fig. 3. Electronic energy loss in Kapton $(C_{22}H_{10}O_5N_2)_n$ as a function of energy for different incident charged particles. (a) ^{9}Be, (b) ^{11}B, (c) ^{12}C, (d) ^{14}N, and (e) ^{16}O.

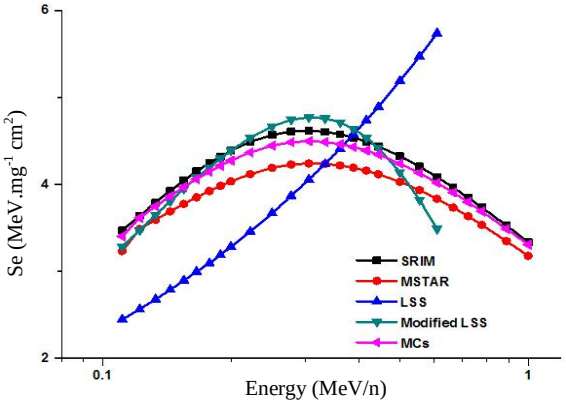

(a)

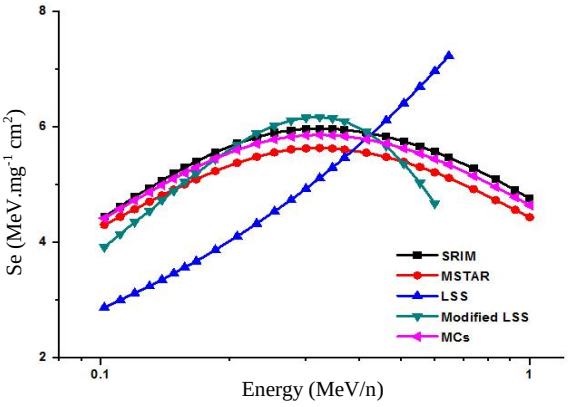

(b)

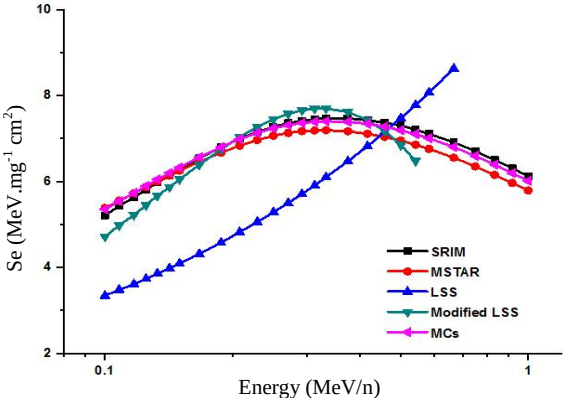

(c)

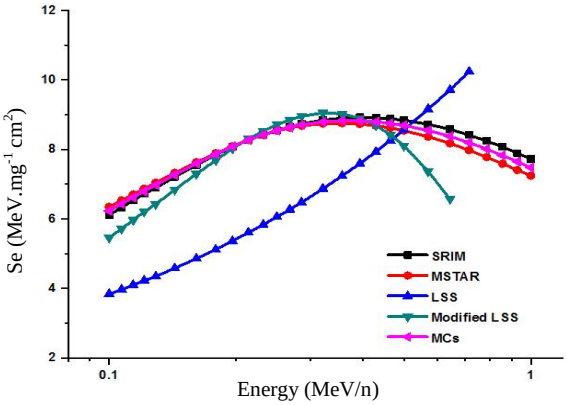

(d)

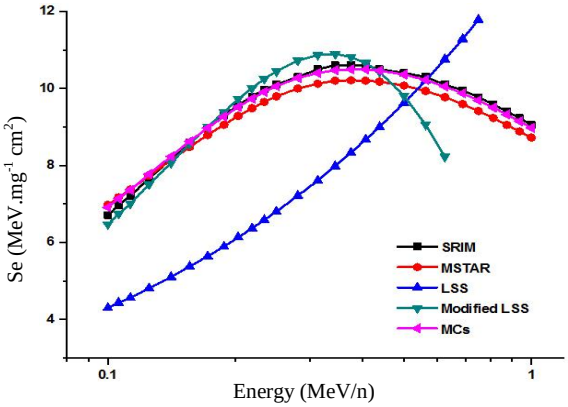

(e)

Fig. 4. Electronic energy loss in LR-115 as a function of energy for different incident charged particles. (a) ^{9}Be, (b) ^{11}B, (c) ^{12}C, (d) ^{14}N, and (e) ^{16}O.

Table 2 presents the electronic stopping power values of LR-115 and Kapton polymers for ^{35}Cl ions in the energy range of ~0.5-1.0 MeV/n, obtained by Monte Carlo simulations and modified LSS theory.

Table 2. Electronic stopping power values based on the Monte Carlo simulations (MCs) and modified LSS theory in LR-115 and Kapton polymeric foils for Cl heavy ion.

Stopping power (MeV mg^{-1} cm^2)						
Target	**Energy (MeV/n)**	**SRIM**	**MSTAR**	**Experimental Results [14]**	**MCs**	**modified LSS theory**
LR-115 $(C_6H_9O_9N_2)_n$	0.5	24.47	23.24	25.52	24.08	26.12
	0.6	24.84	23.61	25.75	24.40	26.27
	0.7	24.98	23.69	25.91	24.51	26.75
	0.8	24.93	23.59	26.01	24.39	25.97
	0.9	24.64	23.41	26.04	24.43	24.46
Kapton $(C_{22}H_{10}O_5N_2)_n$	1.0	24.45	23.19	26.03	23.95	22.56
	0.5	27.45	24.36	24.92	26.03	28.15
	0.6	28.08	24.37	25.09	26.33	28.63
	0.7	28.40	24.30	25.22	26.43	29.01
	0.8	28.39	24.15	25.33	26.34	28.45
	0.9	28.09	23.95	25.40	26.12	26.76
	1.0	27.85	23.71	25.44	25.84	24.45

This table also presents the corresponding electronic stopping power values obtained by SRIM and MSTAR. In order to confirm the validity of calculations in this work, the calculated values of electronic stopping power generated by the presented approach, following Eq. (6), have been compared to those published by P.K. Diwan *et al*., see Ref. [14].

Furthermore, Figs. 5 and 6 illustrate the electronic energy loss of heavy ions ^{9}Be in SiO_2 and ^{16}O in Al_2O_3 as a function of energy. In Fig. 5, we compare our results of electronic stopping power of the SiO_2 crossing by Beryllium at low energy with data obtained by MSTAR data, modified LSS theory and experiment data obtained by Zhang *et al*. [16]. Similar behavior have been observed for Al_2O_3 crossing by oxygen at low energy, the electronic stopping results are compared with MSTAR data, modified LSS theory and experiment data obtained by Pascual-Izarra *et al*. [23], (see Fig. 6). However, we found that, the stopping power values in good agreement with experimental values and MSTAR data by deviation up to 10 %, of SiO_2 and Al_2O_3 materials in the energy range ~0.1-1.0 MeV/n.

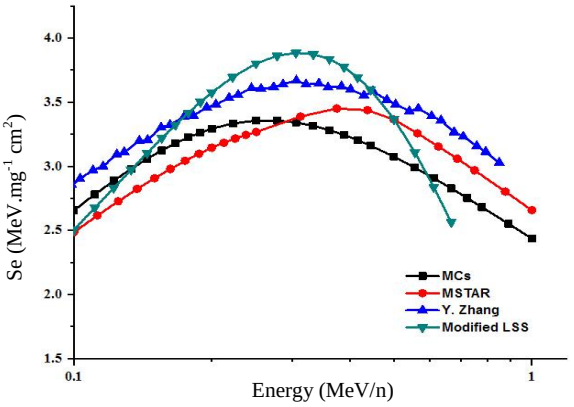

Fig. 5. Electronic energy loss of beryllium in SiO_2 as a function of incident energy.

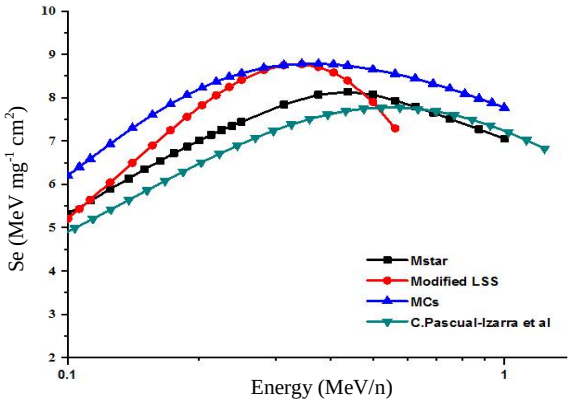

Fig. 6. Electronic energy loss of oxygen in Al_2O_3 as a function of incident energy.

CONCLUSION

We have presented calculation results for the stopping power of ^{9}Be, ^{11}B, ^{12}C, ^{14}N, ^{16}O, and ^{35}Cl in the energy range of interest for Kapton and LR-115 polymeric materials. LSS-theory-based electronic stopping power values, with presently modified ζ and $f(E)$ function, provide close agreement in Kapton and LR-115 for heavy ions with Z_1 = 4-9 and Z_1 = 17, in the energy range of ~0.1-1.0 MeV/n. The modified LSS theory values are in close agreement with Monte Carlo simulations and data from SRIM and MSTAR. Moreover, the stopping power values obtained of Kapton and LR-115 for ^{35}Cl ions are in good agreement with experimental values, SRIM, and MSTAR in the energy range ~0.5-1.0 MeV/n, with deviation generally lower by about 10 %. Good agreement between stopping powers values, MSTAR data ,and experimental results are observed for ^{9}Be in SiO_2 and ^{16}O in Al_2O_3 in the energy range of 0.1-1.0 MeV/n.

AUTHOR CONTRIBUTION

O. El Bounagui, J. El Asri, and H. Erramli equally contributed as the main contributors of this paper. A. Chetaine and N. Tahiri contribute to analysis and / or interpretation of data. All authors read and approved the final version of the paper.

REFERENCES

1. J. Lindhard, M. Scharff and H.E. Schiott, Mat. Fys. Medd. Dan. Vid. Selsk. **33** (1963) 1.
2. H. Erramli and O. El Bounagui, *Charged Particle Activation Analysis: Applications*, in: Encyclopedia of Analytical Chemistry: Applications, Theory and Instrumentation, Wiley Online Library, United Kingdom (2017) 365.
3. O. El Bounagui and H. Erramli, Nucl. Instrum. Meth. Phys. Res. B **268** (2010) 1361.
4. H.A. Bethe, Phys. Rev. **89** (1953) 1256.
5. D. Tahir, Suarga, Yulianti *et al*., Atom Indones. **38** (2012) 100.
6. J.F. Ziegler, J.P. Biersack and U. Littmark, The Stopping and Range of Ions in Solids, Vol. 1. Pergamon Press, New York, (1985) 1.
7. H. Erramli, O. ElBounagui, M.A. Misdaq *et al*., Nucl. Instrum. Meth. Phys. Res. B **263** (2007) 127.
8. U. Fano, Ann. Rev. Nucl. Sci. **13** (1963) 1.
9. L.C. Northcliffe, Ann. Rev. Nucl. Sci. **13** (1963) 67.

10. O. El Bounagui and H. Erramli, Mod. Phys. Lett. B **25** (2011) 2171.
11. L.E. Porter and H. Lin, J. App. Phys. **67** (1990) 6613.
12. H. Geissel, H. Weick, C. Scheidenberger *et al*., Nucl. Instrum. Meth. Res. B **195** (2002) 3.
13. J.M. Fernández-Varea and N.R. Arista, Radiat. Phys. Chem. **96** (2014) 88.
14. P.K. Diwan, V. Sharma, Pratibha *et al*., Nucl. Instrum. Meth. B **266** (2008) 4738.
15. A. Sharma, P.K. Diwan, S. Kumar *et al*., Nucl. Instrum. Meth. B **194** (2002) 7.
16. Y. Zhang, W.J. Weber, D.E. McCready *et al*., App. Phys. Let. **87** (2005) 104103.
17. J. El Asri, O. El Bounagui, N. Tahiri *et al*., Nucl. Technol. **205** (2019) 1236.
18. D.E. Knuth, The Art of Computer Programming (TAOCP), Wesley (1969).
19. W.E. Burcham, Elements of Nuclear Physics, Harlow, Longman (1979).
20. J. Von Neumann, J. Res. Nat. Bur. Stand. Appl. Math. **12** (1951) 36.
21. J. Giber, I. Nagy and J. Laszlo, Nucl. Instrum. Meth. Res. B **2** (1984) 135.
22. W.H. Barkas and M.J. Berger, in Studies in Penetration of Charged Particles in Matter, National Academy of Sciences, National Research Council Publication No. 1133, NAS-NRC, Washington, DC (1967).
23. C. Pascual-Izarra and G. Garcia, Nucl. Instrum. Meth. B **228** (2005) 388.